J. Mater. Environ. Sci. 8 (1) (2017) 78-89
ISSN : 2028-2508
CODEN: JMESCN

Starch as an ecofriendly green inhibitor for corrosion control of 6061-Al alloy

Charitha B.P, and Padmalatha Rao*
Department of Chemistry, Manipal Institute of Technology, Manipal, INDIA

Received 01Jul 2015, Revised 03 Nov 2016, Accepted 10 Nov 2016
**Corresponding author's mail id: padmalatha.rao@manipal.edu*

Abstract
The corrosion inhibition characteristics of biopolymer starch was studied as an ecofriendly inhibitor for the corrosion control of 6061 aluminum alloy in 0.1M HCl. Electrochemical methods such as potentiodynamic polarization (PDP) and electrochemical impedance spectroscopy (EIS) techniques were adopted. Effect of inhibitor concentrations (in the range of 100 to 800ppm) was studied at temperatures of 30, 35, 40, 45 and 50℃. The kinetic and thermodynamic parameters for corrosion and inhibition process were determined. The surface morphology of aluminum in the absence and presence of starch in 0.1M HClsolution was studied using Scanning Electron Microscope (SEM) and Electron Dispersive x-ray spectroscopy (EDX). Suitable mechanism was proposed for corrosion and inhibition process. The percentage inhibition efficiency of starch increased with increasing inhibitor concentrations and also with increase in temperature. Starch acted as a mixed inhibitor, underwent chemical adsorptionand obeyed Langmuir adsorption isotherm.Starch – a biodegradable polymer emerged as a potential, cost effective environmentally begin inhibitor for the corrosion control of 6061-aluminum inHCl.

*Keywords:*6061-Al alloy, Hydrochloric acid, Potentiodynamic polarization, EIS, adsorption isotherm, SEM-EDX

1. Introduction
Aluminum is third most abundant metals found on the earth's crust. Aluminum and its alloys have low atomic weight, high strength to density ratio, high ductility and are excellent conductors of heat and electricity. Because of these properties they are used inaerospace and chemical industries [1-2]. Corrosion resistance of aluminum is due to the formation of naturally formed stable oxide film [3].

Although aluminum has stable oxide film on its metal surface, it undergoes sever pitting corrosion in presence of aggressive medium like hydrochloric acid. Hydrochloric acid is a major industrial chemical, which is widely used for electro-polishing of aluminum [4]Hydrochloric acid is commonly used in pickling and acid cleaning of materials. As a result of this there is remarkable material loss. [5].Hence there is a need of addition of inhibitors to the system where aluminum is in contact with hydrochloric acid. [6].

Organic heterocyclic compounds are used as corrosion inhibitorfor metals in acid medium. Presence of heteroatoms like N, S, O and P usually facilitates the coordination bond formation between metal and the inhibitor. Thus these inhibitors get adsorbed over metallic surface thereby bringing down the rate of corrosion. Unfortunately, some of the synthetic organic compounds are not only costly but also, non-biodegradable and toxic. Due to the adverse effect of these synthetic organic inhibitors on environment and human beings, now-a-days the research activities are geared towards cost-effective, eco-friendly, biodegradable and non-toxic corrosion inhibitors.

Biopolymers are mainly utilized as adhesives, absorbents, lubricants, soil conductors, cosmetics, drug delivery etc. Biopolymers are naturally available cheap, non-toxic and environmentally acceptable and some of them showed to function as effective inhibitors for metal corrosion in different acidic environment [7].

Starch, the bio polymer of present investigation is a principle carbohydrate storage product of higher plants containing 20 to 25% amylose and 75 to 80% amylopectin by weight. Starch is a biodegradable additive or replacement material in traditional oil based commodity plastics [7]. It has wide range of applications in food industry, pharmaceuticals, paper making and many other industrial branches.

As a part of our studies with ecofriendly inhibitors [8, 9, 10]for corrosion control of aluminum, in this present investigation we demonstrate the applicability of biopolymer starch as an inhibitor for the corrosion control of aluminum in hydrochloric acid medium. Starch is chosen because of its environmental and economic benefits.

2. Experimental

2.1.Material

Composition of base alloy is given in the Table 1

Table1. Composition of 6061 Al base alloy

Elements	Cu	Mg	Cr	Si	Al
Composition(%wt)	0.25	1.0	0.20	0.60	balance

2.2. Preparation of test coupon

Cylindrical test coupon of 6061-aluminum alloywith 1cm^2 surface area was sealed with cold setting resin. The exposed flat surface of the mounted part was polished with different grade emery papers (in the range of 200 - 1600). Further polishing was carried with will disc polisher using abrasive i.e. levigated alumina to get the mirror surface. The specimen was then dried and stored in the desiccators for further studies.

2.3. Preparation of medium

The stock solution of HCl of higher concentration was prepared by using 37% HCl and double distilled water. The standardization of HCl was done with standard NaOH solution by volumetric method. From the standard solution, the required concentration of HCl (0.1M) solution was prepared as and when required.

2.4. Preparation of inhibitor solution

Starch (Merck chemicals) was used as such. Molecular weight of the starch was in the range of 110,000 ─ 150,000 Dalton. The concentration of starch was in the range of 100 to 800ppm. The stock solution was prepared by dissolving starch (1g) in boiling water and made up to 1L with 0.1 M hydrochloric acid. The experiments were conducted using a thermostat calibrated up-to ±0.5℃ under unstirred condition.

2.5. Electrochemical studies

Electrochemical measurement of6061- aluminum alloywas carried out by using potentiostat (CH600 D-series, U.S. model with CH-instrument beta software). The electrochemical cell used was a Pyrex glass beaker fitted with three electrodes. Working electrode was 6061- aluminum and reference electrode was saturated calomel electrode. Pt wire was auxiliaryelectrode. Potentiodynamic polarization measurements were done immediately after electrochemical impedance studies without further surface treatment.

Potentiodynamic polarization (PDP) measurements

The finely polished test coupon was immersed in 0.1 M hydrochloric acid containing different concentrations of inhibitor in the temperature range 30 - 50 ^{o}C with 5 °C increment. It was allowed to attain steady state open circuit potential (OCP) for 1800s. The working electrode was polarized to +250mVanodically and −250mVcathodically with respect to OCP at the scan rate of 1mV sec^{-1}and the potentiodynamic current – potential plots were obtained.

Electrochemical impedance spectroscopy (EIS) studies
The EIS studies were done using small amplitude of AC signal of 10mV at the open-circuit potential with a frequency range from 10000 Hz to 0.01 Hz. Nyquist plots were used to analysis of impedance data.In all the above measurements minimum of 3-4 trails were done and average of best three agreeing value was reported.

2.6 Surface morphology studies
Surface morphology study of 6061 Al alloy was carried out by using analytical scanning microscope (JEOL JSM-6380L), in the magnification of 1000X. Surface morphology of the metal sample was obtained by immersing the specimen inhydrochloric acid medium for 2h without and with the addition of inhibitor.

3. Results and discussions

3.1. Fourier transforms infrared (FTIR) spectroscopy of starch
Figure 1.shows the FTIR spectrum of starch.In the fingerprint region between 900 and 1500 cm^{-1}, the absorption bands at 979, 1087, 1164, 1257, 1365, 1465cm^{-1}corresponds to ─C─O─C─, the peak at 1650 cm^{-1} is attributed for tightly bounded H_2O present in starch and the absorption band at 3541 cm^{-1} and 3101 cm^{-1} is attributed for characteristic vibrations of C─H and ─OH bonds.

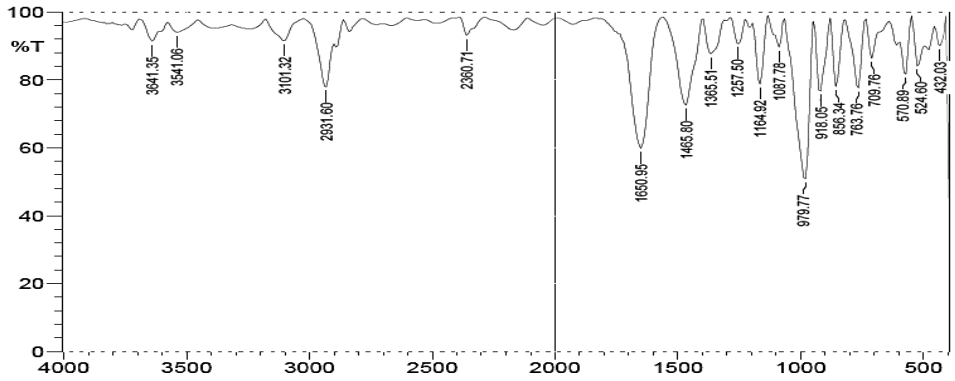

Figure1:FTIR spectrum of starch

3.2. Potentiodynamic polarization (PDP) measurements
The effect of acid concentration on the corrosion rate of aluminum was studied. Figure 2representspotentiodynamicpolarization plotsfor the corrosion of aluminum in 0.1M hydrochloric acid solution at 35℃.in presence of varying concentrations of inhibitor.

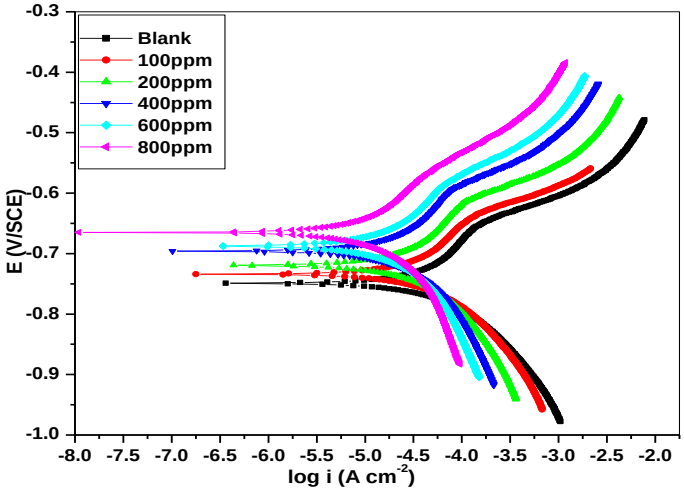

Figure 2: Potentiodynamic polarization curves for the corrosion of 6061-Al alloy in 0.1MHCl containing varying concentrations of inhibitor at 35℃

The useful electrochemical parameters like corrosion current density (i_{corr}), corrosion potential (E_{corr}), anodic slope (β_a) and cathodic slope ($-\beta_c$) were obtained from the polarization studies.
Then the corrosion rate in mmy^{-1} was obtained by using the equation (1)

$$\vartheta_{corr}\,(\text{mmy}^{-1}) = \frac{3270 \times \text{M} \times \text{i}_{\text{corr}}}{\rho \times \text{z}} \qquad (1)$$

where, 3270 is a constant that defines the unit of corrosion rate, ρ is the density of the corroding material (2.7 g cm^{-3}), M is the atomic mass of metal (27) , Z is the electrons transferred/ metal atom (3) [11].
The percentage inhibition efficiency of the inhibitor may be calculated by using the equation (2).

$$I.E.(\%) = \frac{i_{corr} - i_{corr\ (inh)}}{i_{corr}} \times 100 \qquad (2)$$

Table 2 represents the results of potentiodynamic polarization measurement for the corrosion of 6061 aluminum alloy in 0.1Mhydrochloric acid containing varying concentrations of inhibitor at different temperatures.

Table2: Results of potentiodynamic polarization measurements for corrosion of 6061-Al alloy in 0.1MHClcontaining varying concentrations of inhibitor

Temp (℃)	**[Starch] (ppm)**	**E_{corr} (mV vs SCE)**	**i_{corr} (μAcm^{-2})**	**$+\beta_a$ ($mVdec^{-1}$)**	**$-\beta_c$ ($mVdec^{-1}$)**	**CR (mmy^{-1})**	**I.E (%)**
30	Blank	−756	46	683	666	1.09	—
	100	−758	36	767	620	0.91	21.48
	200	−696	33	733	492	0.85	27.58
	400	−758	29	760	639	0.47	36.31
	600	−687	27	720	466	0.34	39.99
	800	−664	26	726	551	0.25	41.72
35	Blank	−744	52	953	662	1.23	—
	100	−734	39	1065	625	0.93	23.96
	200	−719	36	769	557	0.87	30.06
	400	−696	31	733	492	0.49	38.79
	600	−687	30	720	466	0.35	42.47
	800	−665	25	810	473	0.26	51.54
40	Blank	−759	62	786	694	1.46	—
	100	−747	44	989	649	0.95	28.39
	200	−734	41	1055	625	0.88	34.49
	400	−757	35	903	621	0.50	43.22
	600	−698	33	733	492	0.37	46.90
	800	−683	25	694	565	0.28	59.19
45	Blank	−779	107	519	763	1.99	—
	100	−773	76	391	687	0.97	29.40
	200	−775	69	322	656	0.90	35.50
	400	−770	59	321	697	0.52	44.23
	600	−712	56	457	602	0.39	47.91
	800	−696	40	565	604	0.30	62.70
50	Blank	−778	137	478	749	2.27	—
	100	−784	95	562	712	0.99	30.20
	200	−778	87	504	718	0.93	36.30
	400	−777	75	316	677	0.55	45.03
	600	−772	68	918	703	0.41	49.71
	800	−696	50	1063	612	0.32	63.44

It is evident from the table 2, that corrosion current density (i_{corr}) and corrosion rate (CR) decreased with increase in the concentrations of the inhibitor and the I.E(%) increased with increase in the concentrations of the inhibitor. This is mainly because of adsorption of the inhibitor on the surface of the metal. The adsorbed inhibitor molecule creates a protective barrier between the aluminum surface and the aggressive medium. This results in decrease of corrosion rate. There is a slight change in the value of anodic and cathodic slopes. Thecathodic curve in the figure is almost parallel to each other this suggest hydrogen evolution is activated─controlled and it does not alter themechanism of reduction reaction [12].

As per the reported literature [13-14], if the corrosion potential (E_{corr}) value of the inhibited solution is less than±85mV with respect to uninhibited solution, the inhibitor can be considered as distinctively as anodic and cathodic inhibitor. However, in the study the maximum displacement was much less than ±85mV. This suggests that starch may acts as a mixed inhibitor.

3.3.Electrochemical impedance spectroscopy (EIS) measurements

The impedance behavior of starch inhibitor on 6061-Al alloy in 0.1M HCl was studied. The data obtained from EIS studies gives the information about the type of electrochemical process occurred at electrode/electrolyte interface. Figure 3 is the Nyquist plot for the corrosion control of 6061-Al at 35 ℃ in the corrosive medium and along with the presence of different concentration of starch inhibitor. In the figure, the impedance plots showed semicircle, which highlights that; corrosion is mainly controlled by charge transfer process. In the figure, the high frequency (HF) region and low frequency (LF) region corresponds to large and small capacitive loop respectively. Similar Nyquist plots have been reported in the literature for the corrosion control of 6061 Al alloys in HCl medium [15–21]. The large capacitive loop at HF region corresponds to transfer of charge during corrosion process and development of protective oxide film [22, 23]

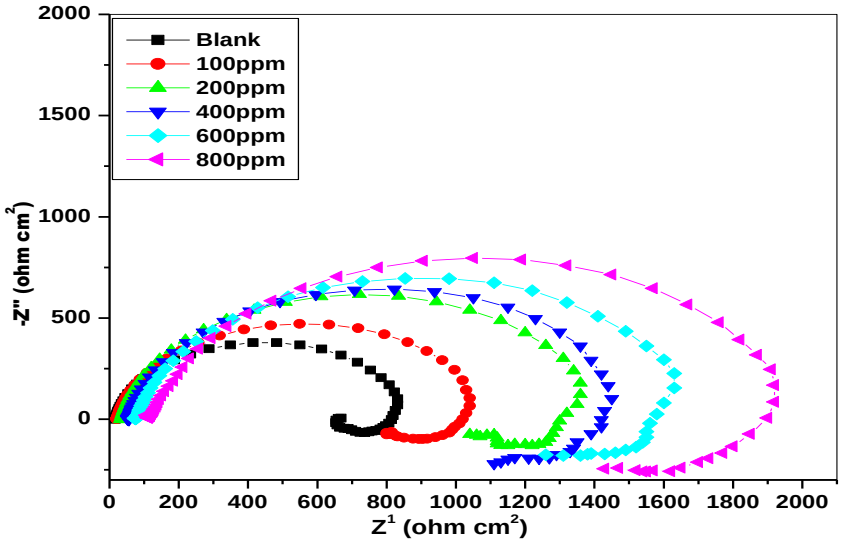

Figure3: Nyquist plot for corrosion of 6061-Al alloy in 0.1MHClcontaining varying concentrations of inhibitor at 35℃

The Nyquist plot obtained for the corrosion control of 6061-Al alloy is showing depressed semicircular impedance spectra with the addition of starch inhibitor and it also found that the diameter of the capacitive loop increased with increase in the inhibitor concentration, this increase in the diameter is due to decrease on the corrosion rate by the adsorption of the inhibitor molecule onto the surface of the metal.

Figure 4 is the equivalent circuit of nine elements which was used to simulate the impedance plot for 6061-aluminum alloy.

The equivalent circuit consists of nine elements. They are solution resistance (R_s)and charge transfer resistance (R_{ct}) , inductive resistance (R_L)and the inductive element (L). The CPE (constant phase element, Q)is parallel to the series of capacitors C_1 and C_2 and alsoparallel to the series of resistor R_1, R_2, R_L and R_{ct}. R_L is parallel to L

inductor. The parallel circuit of a resistor is attributed for oxide film due to the ionic conduction in the oxide film and the capacitance due to its dielectric properties.

The double layer capacitance (C_{dl}) and polarization resistance (R_p) can be calculated by using the equations,

$R_p = R_1 + R_2 + R_L + R_{ct}$ (3)

$C_{dl} = C_1 + C_2$ (4)

The zimpwin software of version 3.21 was used for circuit fitment.

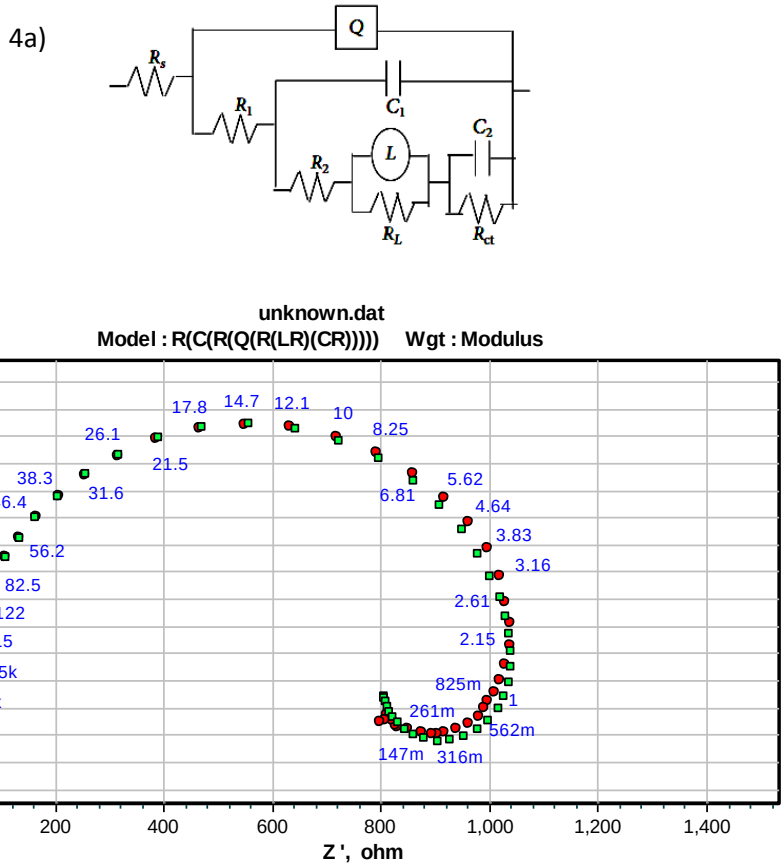

Figure 4: a) Equivalent circuit used to fit the experimental EIS data and b) simulated plot obtained for the corrosion of 6061 aluminum alloy in 0.1MHClat 35℃

Table 3 represents results obtained. The components Q_{dl} and co-efficient 'a' of CPE quantifies different physical phenomena such as surface roughness due to surface inhomogeneous, adsorption of inhibitor, porous layer formation etc [24]. The different physical phenomena like surface in-homogeneousness which results from the surface roughness are quantified by these parameters. [25].

$C_{dl} = Q_{dl} \times (2\pi f_{max})^{(a-1)}$ (5)

The polarization resistance (R_P) values are varies inversely with corrosion current density (i_{corr}). The inhibition efficiency was obtained using equation (6)

$$I.E.(\%) = \frac{R_{P(inh)} - R_P}{R_{P(inh)}} \times 100 \quad (6)$$

R_P and $R_{P(inh)}$ are the polarization resistance in the absence and in the presence of the inhibitor [26, 27]. R_P values increased with increase in the concentration of the inhibitor. This results in lowering the value of double layer capacitance (C_{dl})[28].

Table 3: Results of EIS studies for corrosion of 6061 Al-alloy in 0.1MHCl

Temp (℃)	[Starch] ppm	C_{dl} ($\mu F\ cm^{-2}$)	R_p ($\Omega\ cm^2$)	I.E (%)
30	Blank	25	698	—
	100	24	873	20.04
	200	22	996	29.19
	400	21	1054	33.77
	600	19	1175	40.59
	800	18	1259	44.55
35	Blank	36	515	—
	100	34	669	23.01
	200	32	743	30.68
	400	28	849	39.34
	600	27	889	42.06
	800	25	1056	51.23
40	Blank	42	469	—
	100	40	648	27.62
	200	38	751	37.54
	400	35	832	43.62
	600	33	876	46.46
	800	30	1173	60.01
45	Blank	56	314	—
	100	53	444	29.27
	200	49	469	33.04
	400	45	558	43.72
	600	43	654	51.98
	800	40	895	64.91
50	Blank	68	259	—
	100	56	361	28.25
	200	53	398	34.92
	400	47	456	43.20
	600	44	506	48.81
	800	41	698	62.89

3.4. Effect of temperature

The inhibition efficiency of the inhibitor increased with increase in temperature. This increase in inhibition efficiency may be due tofirmadsorption of the inhibitor molecule on the metal surface [29]. The energy of activation (E_a)was calculated using Arrhenius law equation (7)

$$\ln (CR) = B - \frac{E_a}{RT} \quad (7)$$

where, B is Arrhenius constant which depends upon the type of metal and R is universal gas constant (8.314 $JK^{-1}mol^{-1}$), T is the absolute temperature. Figure 5 depicts Arrhenius plot for the standard system.The plots of ln (CR) verses 1/T gave straight line with a slope (slope = $-E_a/R$) from which energy of activation (E_a) for the corrosion and the inhibition process was calculated.

The transition state equation was used to calculate the enthalpy (ΔH_a) and entropy of activation (ΔS_a) for the metal dissolution and inhibition process. The transition state equation (8)[30]

$$CR = \frac{RT}{Nh}\exp(\frac{\Delta S_a}{R})\exp(-\frac{\Delta H_a}{RT}) \quad (8)$$

where h is planks constant, N is Avogadro's number. Figure 6 .is the plot of ln (CR/T) verses 1/T for aluminum in various concentration of inhibitor in 0.1Mhydrochloric acid. The plot of ln (CR/T) verses 1/T gave a straight line with slope (slope = $-\frac{\Delta H_a}{R}$); and the intercept (intercept = $\ln(R/Nh) + \frac{\Delta Sa}{R}$) which gave the values of enthalpy of activation and entropy of activation respectively. Activation parameters for the corrosion of aluminum in 0.1Mhydrochloric acidcontaining different concentrations of inhibitors are tabulated in Table 4.

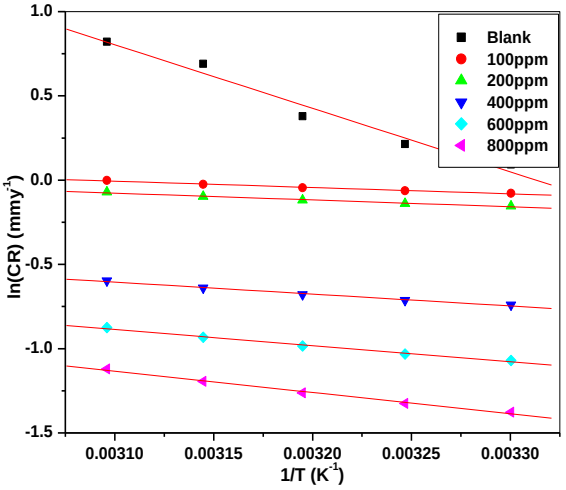

Figure 5: Arrhenius plot for corrosion inhibition of aluminum in 0.1MHClcontaining different concentration of inhibitors

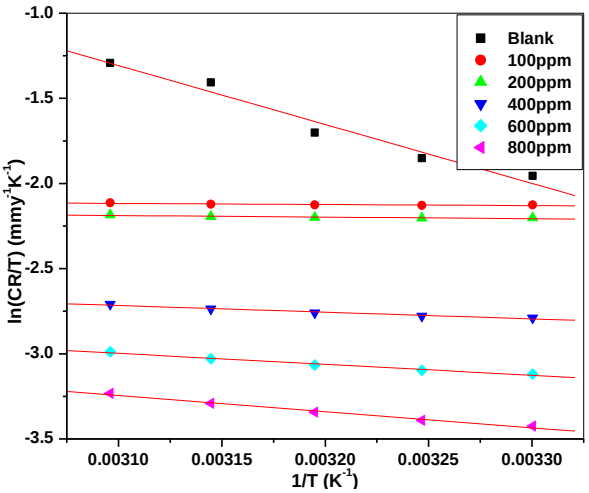

Figure 6: Plots of ln(CR/T) vs 1/T for the corrosion of aluminum in 0.1M HCl containing varying concentration of inhibitors

Table 4: Activation parameters for the corrosion of aluminum in 0.1M HCl at various concentrations of inhibitor

[Starch] g L^{-1}	E_a (kJmol^{-1})	ΔH_a (kJmol^{-1})	ΔS_a (Jmol^{-1}K^{-1})
Blank	31.3	28.77	− 188.1
100	3.12	0.527	−199.4
200	3.36	0.766	−199.4
400	5.86	3.269	−199.0
600	7.95	5.348	−198.5
800	10.4	7.876	−197.8

Energy of activation (E_a)values of the uninhibited solutions were higher when compared with that of inhibited solution. This decrease in the $E_a$value of the inhibited solution is suggestive of chemical adsorption of the inhibitor on the surface of the metal. The adsorbed molecules on the metal surface allow charge transfer during the corrosion process, thereby leading to increase in energy of activation. In the other words, the inhibitor molecule gets chemically adsorbed on the metal surface and reduces the electrochemical corrosion process [31,32, 33]. The entropy of activation (ΔS_a) values are negative which indicates that, the activated complex in rate determining step is an dissociation rather than association i.e., decrease in the disordernesswhich leads to the formation of activated complex [34, 35].

3.5. Adsorption isotherm

A phenomenon of adsorption plays a vital role in deciding the mechanism of inhibition process. From percentage inhibition efficiency, the surface coverage (θ) be calculated using the equation (9)

$\theta = I.E.(\%)/100$ (9)

Off the different adsorption models, the experimental data was found to best fit for Langmuir adsorption isotherm, θ is related C_{inh}as given by equation (10)

$\frac{C}{\theta} = \frac{1}{K} + C$ (10)

The plot of C/θ verses C gave a straight line with intercept K. 'K' represents the adsorption/ desorption equilibrium constant. Adsorption plot is given in the Figure 7.

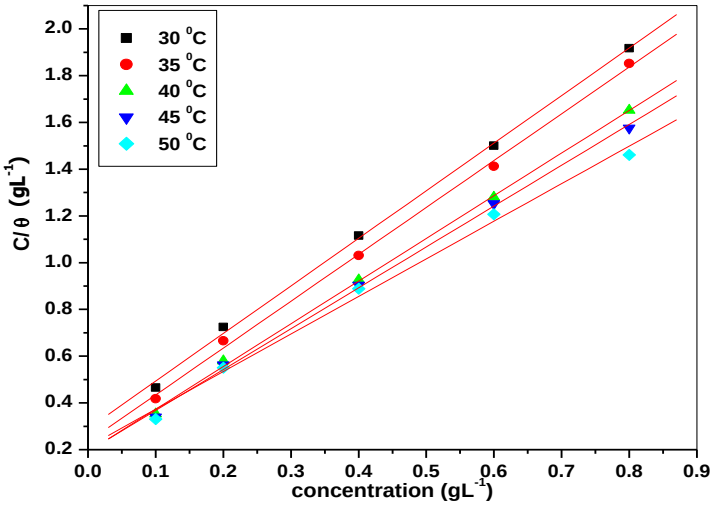

Figure 7: Langmuir adsorption isotherm for the adsorption of starch on 6061-Al alloy in 0.1M HCl at different temperatures

The standard free energy of adsorption (ΔG^0_{ads}) is related to adsorption /desorption constant (K)by the following equation,

$K = \frac{1}{C_{water}} \exp(-\Delta G^0_{ads} / RT)$ (11)

where R is universal gas constant, T is the absolute temperature; as the concentration of water has unit gL^{-1} and K has unit Lg^{-1} the value will become approximately 1000 [36].

The table 5 shows the thermodynamic parameters for the adsorption of inhibitor on the surface of the metal. As per reported literature [37, 38] standard free energy of adsorption($-\Delta G^0_{ads}$)values around $-20 kJmol^{-1}$ or lower are consistent with electrostatic interaction between the charged inhibitor species and the charged metal (physisorption). The more negative than $-40 kJmol^{-1}$ involve sharing of charge or transfer of charge from the inhibitor molecule to the metal surface to form a coordinate bond (chemisorptions). In the present investigation, the calculated standard free energy of adsorption($-\Delta G^0_{ads}$) values areless than $-20 kJmol^{-1}$. This indicates that adsorption of inhibitor molecule on the metal surface is predominately due to physisorption. Thestandard enthalpy of adsorption(ΔH^0_{ads}) and standard entropy of adsorption (ΔS^0_{ads}) values are obtained by plotting a graph of ΔG^0_{ads} verses T.

The graph was linear with standard enthalpy of adsorption (ΔH^0_{ads})and the slope corresponding to standard entropy of adsorption (ΔS^0_{ads}). The negative value of ΔH^0_{ads} shows that the adsorption of inhibitor is an exothermic process. Generally, an exothermic process signifies eitherphysisorption or chemisorption. In an exothermic process, if standard enthalpy of adsorption value is lower than $-40 kJmol^{-1}$ then interaction of the inhibitor molecule is mainly through physical adsorption process and if value is more than-100 $kJmol^{-1}$then the process is chemisorptions[39]. Here, the value ΔH^0_{ads} is 11.98 kJ mol^{-1}which supports the chemical adsorption of inhibitor molecule on the surface of the metal.Thermodynamic parameters are listed in the Table 5.

Table 5: Thermodynamic parametersfor the corrosion of aluminum in 0.1MHCl

Temperature (K)	$-\Delta G^0_{ads}$ ($kJmol^{-1}$)	ΔH^0_{ads} ($kJmol^{-1}$)	ΔS^0_{ads} ($k\ Jmol^{-1}K^{-1}$)
303	20.52		
308	21.45		
313	22.16	11.98	0.108
318	22.47		
323	22.74		

3.5. Explanation for inhibition

Aluminum is protected by oxide film of amorphous γ-alumina. In the neutral aqueous solution the oxide film thickens and forms crystalline hydrated alumina layer. In the acidic medium, the dissolution of the metal takes place as follows,

$Al_{(s)} + H_2O \leftrightarrows AlOH_{ads} + H^+ + e^-$ (12)

$AlOH_{ads} + 5H_2O + H^+ \leftrightarrows Al^{3+}.6H_2O + 2e^-$ (13)

$Al^{3+} + H_2O \leftrightarrows [AlOH]^{2+} + H^+$ (14)

$[AlOH]^{2+} + X^- \leftrightarrows [AlOHX]^+$ (15)

Thus, dissolution of metal takes place by the soluble complex ion formed. The cathodic reaction involves the hydrogen gas evolution:

$H^+ + e^- \rightarrow H_{(ads)}$ (16)

$H_{(ads)} + H_{(ads)} \rightarrow H_2$ (17)

Evaluation of kinetic as well as thermodynamic parameters suggests the possibility of chemical adsorption on the surface of the metal. At all studied temperatures value of standard free energy of adsorption (ΔG^0_{ads})were more than – 20 kJ mol^{-1}, supporting the chemical adsorption process. The mechanism of chemical adsorption may be explained as follows:

Structure of starch molecule is given in Figure 9. It consists of two polymeric units, amylose and amylopectin. Amylose is a helical, non-branched polymer consisting of $\alpha - 1,4$ linked D─ glucose monomer and amylopectin is a highly branched polymer consisting of both $\alpha - 1,4$ and $\alpha - 1,6$ linked D─ glucose monomers [40]

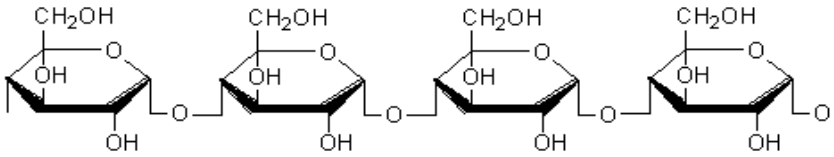

Figure 9(a): Structure of amylose.

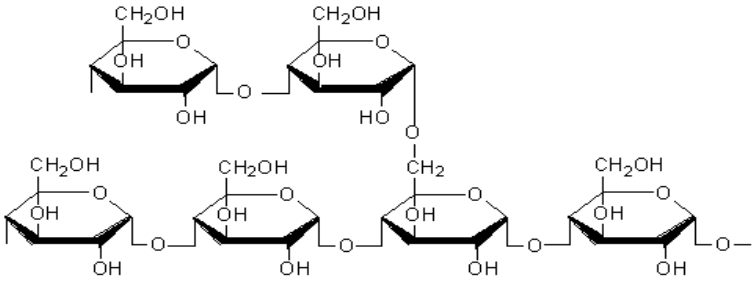

Figure9(b): Structure of amylopectin

Starch molecule is giant molecule and it contains plenty of – OH groups.The presence of π─electrons and lone pair of electrons on oxygen atom are involved in protecting Al surface undergoing corrosion. The electrons are donated to the vacant p─orbitals of Al which leads to the formation of co─ordinate bond between the metal

surface and inhibitor molecule, as the metal get protected by forming co─ordinate bond with inhibitor molecule, it can be suggest the chemical adsorption of the inhibitor molecule.
Thus a protective barrier will be formed between the metal and corrosive and the starch effectively control the corrosion process. The formation of smooth film over the surface of the metal is supported by surface morphology studies using SEM.

Surface morphology studies
The SEM image of freshly polished 6061─Al material is shown in the figure 10(a), this image shows smooth surface of the alloy with few scratches. SEM image of the sample in contact with 0.1M hydrochloric acid is shown in Fig 10(b). When the Surface of 6061─Al alloy was observed in higher magnification its surface seems to be rough due to the formation of pits. Here, 6061-Alis highly susceptible to undergo inter-granular corrosion. This is due to the presence of magnesium in the alloy. In presence of corrosiveenvironment formation of Al_3Mg_2 takes place at grain boundaries and leads to inter-granular corrosion [43]. It is evident that, after the addition of inhibitor the surface has become smooth. Fig 10(c) shows the smooth surface of 6061─Al. This is mainly because of the formation of inhibitor film on the surface of the metal.

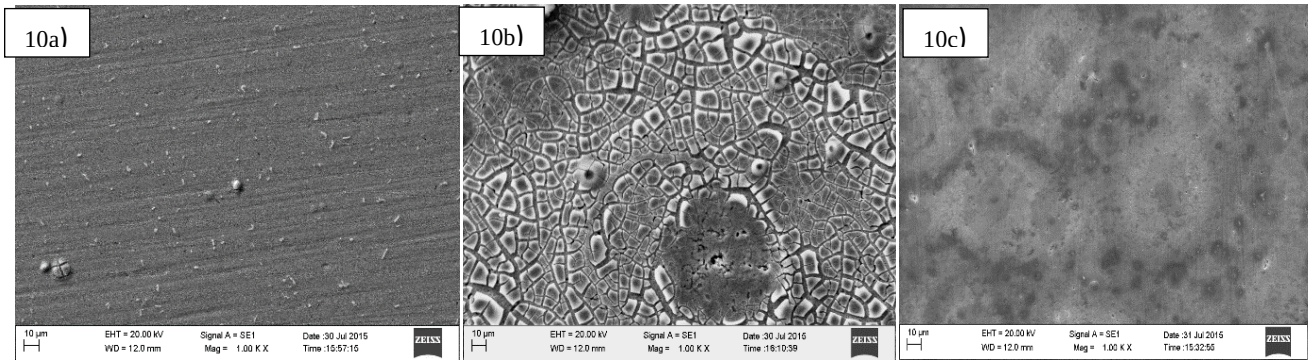

Figure 10: SEM image of 6061 Al alloy of a) freshly polished surface, b) immersed in 0.05 M HCl medium, c) immersed in 0.05 M HCl medium + 800ppm starch at 30℃

EDX spectrum corresponds to un-corroded, corroded and inhibited samples were analyzed. The data of elemental mapping is given in the Table 6. Increase in % composition of oxygen and chlorine in the corroded sample is indicative of dissolution of stable oxide film layer. Peak due to carbon in the inhibited sample confirms the adsorption of starch on the surface of the material.

Table 6: EDX data obtained for 6061Al surface analysis

Samples	**(%) Composition**			
	Al	**O**	**Cl**	**C**
Freshly polished 6061Al alloy	80.18	4.03	---	---
Specimen immersed in 0.1M HCl medium	41.29	24.36	1.57	---
Specimen + 0.1M HCl + 800ppm starch	62.31	4.05	---	33.64

Conclusions

1. Starch can be considered an effective ecofriendly corrosion inhibitor.
2. I.E.(%) of starch increased with increase in concentrations of inhibitor and with increase in temperature.
3. Starch acted as a mixed inhibitor by bringing down both thecathodic and anodic reaction under control.
4. Starch adsorbed over the surface of metal through chemisorption and obeyed Langmuir adsorption isotherm.
5. Starch emerged as a potential biopolymer, which is not only biodegradable but also has economic benefits.
6. Results obtained by potentiodynamic polarization method and electrochemical impedance spectroscopy method were in good agreement with one another.

Acknowledgement: Ms. Charitha B P is gratefulto Manipal University for Research Fellowship and Department of Chemistry M.I.T. Manipal for laboratory facilities

References:

1. Roberts J. D., and Caserio M.C., W.A Benjamin Inc., California, (1979).
2. Stansbury E. E., Buchanan R. A., ASM international materials park, USA (2000).
3. Vereceken J, *Talat lecturers,* 6 (1994) 5103.
4. Vargel C., Corrosion of Aluminium. Elsevier, UK, (2004).
5. Amin M.A., Mohsen Q., Hazzai O.A., *Mater. Chem. Phys.*114 (2009) 908.
6. Andreatta F., Lohrengel M., Terryn H and de witJHW., *Electrochemica Acta.* 48 (2003) 3239
7. US congress, office of technology assortment, Biopolymers: making materials nature's way, (1993)
8. Deepa prabhu, Padmalatha Rao, *J. Envi. Chem. Eng.*, 1 (2013) 676.
9. Deepa prabhu, Padmalatha, *Int. Chem. Tech. Research*, 5 (2013) 2690
10. Deepa prabhu, Padmalatha Rao, *Intl. J. Corr.* (2013),13 pages
11. Fontana MG., Corrosion engineering, McGraw-hill, Singapore, 3 (1987)
12. Rosliza R., Senin H.B., Wan Nik W.B., *Colloids Surf.* 312 (2008) 185.
13. Ferreira E.S., Giancomelli C., Giacomelli F.C., Spinelli A., *Mater. Chem. Phys*. 83 (2004) 129
14. Li WH., He Q., Pei C.L., Hou B.R.,*J. Appl. Electrochem*, 38 (2008) 289.
15. Metikos-Hukovic M., Babic R., Grubac Z., *J. Appl. Electrochem.* 28 (1998) 433
16. Brett, C.M.A., *J. Appl. Electrochem*. 20 (1990) 1000
17. Lee E.J., Pyun S.I., *Corros. Sci.* 37 (1995) 157
18. Brett, C.M.A., *Corros. Sci*.33 (1992) 203
19. Khaled K.F., Al-Qahtani M.M., *Mater. Chem. Phys.*, 113 (2009) 150
20. Frers, M.M. Stefenel, Mayer C., Chierchie T., *J. Appl. Electrochem.* 20 (1990) 996
21. Mansfeld F., Lin S., Kim K., Shih H., *Corros. Sci.*, 27 (1987) 997.
22. Mansfeld F., Lin S., Kim S., Shih H., *Werkstoffe und Korrosion*, 39 (1988) 487.
23. Umoren S.A., Obot I.B., Ebenso E.E., Okafor P.C., *Anti-Corros. Meth. Mater.* 53 (2006) 277
24. Rivera-Grau LM., Casales M., Regla I., Ortega-Toledo D.M., Ascencio-Gutierrez J.A., Porcayo Calderon J., Martinez-Gomez L., *Int. J. Electrochem. Sci.*, 8(2013) 2491.
25. Pinto GM., Nayak J., Nityananda Shetty A., *Mater. Chem. Phys*. 125 (2011) 628
26. Sanatkumar B.S., Nayak J., Shetty A.N., *J. Coat. Technol. Res.* 4 (2011) 483.
27. Abdel-Gaber A.M, Abd-El-Nabey B.A., Sidahmed I.M., El-Zayady A.M., Saadawy M. *Corros. Sci.* 48 (2006) 2765.
28. Poornima T., Jagannatha N., Nityananda Shetty A., *Portugal, Electrochim. Acta.* 28 (2010) 173.
29. Ashish Kumar Singh M.A., Quraishi M.A.,*Corros. Sci.* 52 (2010) 152.
30. Bouklah M., Hammouti B., Aounti A., BenhaddaT., *Prog. Org. Coat.* 49 (2004) 225.
31. Ashassi-Sorkhabi H., Shaabani B., Seifzadeh D., *Appl. Surf. Sci.* 239 (2005) 154.
32. Osman M.M., El-Ghazawy R.A., Al-Sabagh A.M., *Mater. Chem. Phys.* 80 (2003) 55.
33. Mansfeld F., Corrosion Mechanism, Marcel Dekkar, New York,119 (1987).
34. Sahin M., Bilgic S., Yilmaz H.,*Appl. Surf. Sci.* 195 (2002) 1
35. Ateya B., El-Anadouli B. E., El-Nizamy F. M., *Corros. Sci.* 24 (1984) 509
36. Xianghong Li., Shuduan Deng., *Corros. Sci*. 65 (2012) 299
37. Hosseini M., Mertens S.F.L., Arshadi M.R., *Corros Sci.* 45 (2003) 1473
38. Ehteshamzadeh M., Shahrabi T., Hosseini M., *Anti. Corros. Meth. Mater.* 53 (2006) 296
39. Zarouk A., Hammouti B., Zarrok H., Al-Deyab S.S., Messali M., *Int. J, Electrochem, sci*. 6 (2011) 6261
40. Kulkarni Vishakha S., Butte Kishore D, Rathod Sudha S., *Int. Res. Pharm. Biomed. Sci.*, 3 (2012) 1597
41. www.nace.org/Corrosion-Central/Corrosion-101/Intergranular-Corrosion/